Antifungal *Pisum sativum* Defensin 1 Interacts with *Neurospora crassa* Cyclin F Related to the Cell Cycle†

Denise S. Lobo,‡,§ Iuri B. Pereira,‡ Lucianne Fragel-Madeira,|| Luciano N. Medeiros,‡ Luiz M. Cabral,‡ Jane Faria,⊥ Maria Bellio,# Reinaldo C. Campos,§ Rafael Linden,|| and Eleonora Kurtenbach*,‡

Instituto de Bioquímica Médica, Instituto de Biofísica Carlos Chagas Filho, Instituto de Ciências Biomédicas, and Instituto de Microbiologia Prof. Paulo de Góes, Universidade Federal do Rio de Janeiro, Centro de Ciências da Saúde, 21941-590 Rio de Janeiro-RJ, Brazil, and Departamento de Química, Pontifícia Universidade Católica do Rio de Janeiro, Rua Marquês de São Vicente 225 Gávea, 22453-900 Rio de Janeiro-RJ, Brazil

Received July 17, 2006; Revised Manuscript Received November 4, 2006

ABSTRACT: Plant defensins, components of the plant innate immune system, are cationic cysteine-rich antifungal peptides. Evidence from the literature [Thevissen, K., et al. (2003) *Peptides 24*, 1705−1712] has demonstrated that patches of fungi membrane containing mannosyldiinositolphosphorylceramide and glucosylceramides are selective binding sites for the plant defensins isolated from *Dahlia merckii* and *Raphanus sativus*, respectively. Whether plant defensins interact directly or indirectly with fungus intracellular targets is unknown. To identify physical protein−protein interactions, a GAL4-based yeast two-hybrid system was performed using the antifungal plant peptide *Pisum sativum* defensin 1 (*Ps*d1) as the bait. Target proteins were screened within a *Neurospora crassa* cDNA library. Nine out of 11 two-hybrid candidates were nuclear proteins. One clone, detected with high frequency per screening, presented sequence similarity to a cyclin-like protein, with F-box and WD-repeat domains, related to the cell cycle control. GST pull-down assay corroborated *in vitro* this two-hybrid interaction. Fluorescence microscopy analysis of FITC-conjugated *Ps*d1 and DAPI-stained fungal nuclei showed in vivo the colocalization of the plant peptide *Ps*d1 and the nucleus. Analysis of the DNA content of *N. crassa* conidia using flow cytometry suggested that *Ps*d1 directed cell cycle impairment and caused conidia to undergo endoreduplication. The developing retina of neonatal rats was used as a model to observe the interkinetic nuclear migration during proliferation of an organized tissue from the S toward the M phase of the cell cycle in the presence of *Ps*d1. The results demonstrated that the plant defensin *Ps*d1 regulates interkinetic nuclear migration in retinal neuroblasts.

Plant defensins, innate components of the plant immune system, are cationic antimicrobial peptides. These defensins present a wide yet distinctive antifungal and/or antibacterial spectrum of activity, suggesting their application as natural antimicotics and/or antibiotics (*1*). The disulfide-linked cysteines specifically distributed in their sequence stabilize their tertiary structure with two antiparallel β-sheets in the peptide's N- and C-termini characteristic of defensins found in other types of organisms, including insects and humans (*2*, *3*). In their tertiary structure, diverse families of cationic antimicrobial peptides contain segregated clusters of charged and hydrophobic regions that could be specific for their membrane permeability and/or membranolytic properties.

Recently, our group isolated and characterized two plant defensins from the garden pea, *Pisum sativum* defensins 1 and 2, with 46 and 47 amino acids, respectively. Both peptides were highly expressed in seeds and leaves of *P. sativum* and showed antifungal activity against *Neurospora crassa*, *Aspergillus niger*, *Aspergillus versicolor*, and *Fusarium solani* but not *Saccharomyces cerevisiae* (*4*). Total plant mRNA content analysis showed that *P. sativum* defensin 1 (*Ps*d1)[1] was expressed constitutively, while expression of *P. sativum* defensin 2 (*Ps*d2) was induced in response to fungal infection. Thus, we cloned *Ps*d1 cDNA and described

† This work was supported by grants from Conselho Nacional de Desenvolvimento Científico e Tecnológico (CNPq), Fundação de Amparo a Pesquisa do Estado do Rio de Janeiro Carlos Chagas Filho (FAPERJ), and Coordenação de Aperfeiçoamento de Pessoal de Nível Superior (CAPES).

* To whom correspondence should be addressed. Tel: 55-21-25626753. Fax: 55-21-25626754. E-mail: kurten@bioqmed.ufrj.br.

‡ Instituto de Bioquímica Médica, Universidade Federal do Rio de Janeiro.

§ Departamento de Química, Pontifícia Universidade Católica do Rio de Janeiro.

|| Instituto de Biofísica Carlos Chagas Filho, Universidade Federal do Rio de Janeiro.

⊥ Instituto de Ciências Biomédicas, Universidade Federal do Rio de Janeiro.

Instituto de Microbiologia Prof. Paulo de Góes, Universidade Federal do Rio de Janeiro.

[1] Abbreviations: *Ps*d, *Pisum sativum* defensin; *Rs*AFP, *Raphanus sativus* antifungal peptide; *Dm*AMP, *Dahlia merckii* antimicrobial peptide; FGSC, Fungal Genetic Stock Center; FITC, fluorescein isothiocyanate; DAPI, 4,6-diamidino-2-phenylindole; PI, propidium iodide; BrdU, 5-bromo-2-deoxyuridine; 3-AT, 3-aminotriazole; SD, synthetic dropout culture medium; PD, potato dextrose culture medium; PBS, phosphate-buffered saline solution, pH = 7.4; X-gal, 5-bromo-4-chloro-3-indolyl β-D-galactopyranoside; OD, optical density; IPTG, isopropyl β-D-thiogalactopyranoside; GST, glutathione *S*-transferase; MTs, microtubules; OCT, optimal cutting compound; NBL, neuroblastic layer; *e*-value, expect value or background noise; FACS, fluorescent activated cell sorter.

10.1021/bi061441j CCC: $37.00
Published on Web 01/06/2007

the use of the *Pichia pastoris* expression system for high-level laboratory-scale production of *Ps*d1 (*5*). NMR spectra of both native and recombinant *Ps*d1 indicated that both are folded in a nearly identical manner. The eight cysteine residues in both recombinant and native *Ps*d1 primary structure participated in the formation of the four disulfide bridges characteristic of their $\beta\alpha\beta\beta$ tertiary structure (*5*, *6*). This functional recombinant antifungal peptide *Ps*d1 was used in the in vivo experiments described in this study.

Regarding the mode of action of plant defensins, it has been shown that *Dm*AMP1 and *Rs*AFP2, isolated from *Dahlia merckii* and from *Raphnus sativum*, respectively, induced a variety of rapid fungal membrane responses (*7*). Alterations such as membrane permeabilization, resulting in increased Ca^{2+} uptake and K^+ efflux, alkalinization, and changes in membrane potential suggested plant defensin interaction with the fungal membrane (*8*, *9*). Thevissen and co-workers (*10*) studying plant defensin fungal membrane binding sites for *Dm*AMP1 and *Rs*AFP2 identified certain sphingolipids in the plasma membrane of different fungi that selectively interacted with these plant defensins. They found that *Dm*AMP1 antifungal sensitivity was correlated to the level of mannosyldiinositolphosphorylceramide in the membrane of yeast strains, demonstrating the role of complex sphingolipids in *Dm*AMP1 antifungal activity (*11*, *12*). However, the interaction of radish defensin *Rs*AFP2 with fungal membrane glucosylceramides was shown to be a necessary but not sufficient condition for the inhibition of the fungal growth, suggesting that other targets may be involved in the mechanism by which plant defensins inhibit fungal growth (*13*). A major question is how the complex lipid−plant defensin interaction leads to the antifungal membranolytic properties or to the internalization process of the plant defensin and intracellular effects. Yet no intracellular targets related to the antifungal activity of plant defensins have been identified in fungi.

The aim of this work is to investigate intracellular mechanisms of action of the plant peptide *Ps*d1. The yeast two-hybrid screening system was used to identify direct protein−protein interactions between the *Ps*d1 peptide and the fungal proteins. The system consisted of the *Ps*d1 peptide as bait and a *N. crassa* cDNA library as possible targets.

Target cDNA inserts from the expression library that encode target proteins detected by the two-hybrid technique were identified in the *N. crassa* databases. Nine out of 11 candidates presented sequence similarities to nuclear proteins. Fluorescence microscopic analysis corroborated the two-hybrid result as FITC-labeled *Ps*d1 reached the nucleus of the filamentous fungus *F. solani*. One of the two-hybrid interacting clones encoded a *N. crassa* cyclin F related to the control of the cell cycle. GST pull-down assay confirmed this interaction.

Flow cytometric analysis of *N. crassa* conidia showed a temporal increase of the conidial DNA content in the presence of *Ps*d1 without subsequent completion of cell division. This result pointed to the fact that *Ps*d1 affects the normal progression of the cell cycle.

Bai and co-workers (*14*) first described the human cyclin F and a yeast cyclin, CLB4, by genetic selection designed to identify human and yeast genes capable of suppressing temperature-sensitive yeast mutants of Cdc4, a protein required for entry into the S-phase. The human cyclin F begins to accumulate in the S phase, peaks in the G2 phase, and declines during mitosis (M phase) (*14*, *15*).

The developing retina of neonatal rats is an ideal model that can be used to study accurately the cell cycle, including the transitions from S-phase to G2-phase and from G2-phase to the M-phase (*16*). The cell cycle along the proliferating zone proceeds in synchrony with a controlled interkinetic nuclear migration from the innermost to the outermost stratum of the long neuroblastic layer. We observed an inhibitory effect of this spatial and temporal distribution of nuclei on the presence of the plant defensin *Ps*d1. The results showed that the action mechanism of the cationic antifungal plant peptide *Ps*d1 involves nuclear targets.

EXPERIMENTAL PROCEDURES

Rationale. This project used a four-step approach to show that plant defensin *Ps*d1 interacts with the nucleus. Initially, the yeast two-hybrid system was used to screen a *N. crassa* cDNA library for proteins that directly interacted with *Ps*d1 as "bait". The pull-down assay using GST-fused two-hybrid candidate cyclin F and [^{35}S]methionine *Ps*d1 peptide confirmed the two-hybrid interaction in vitro. This was followed by fluorescence microscopic analysis in vivo of FITC-conjugated *Ps*d1 peptide and DAPI-stained *F. solani* hyphal nuclei colocalization. Additionally, fluorescent activated cell sorter (FACS) analysis of the DNA content of *N. crassa* germinating conidia in the presence of *Ps*d1 showed that *Ps*d1 affected the mitotic cell cycle. Finally, we tested the action of *Ps*d1 peptide on interkinetic nuclear migration in the developing mammalian retina during the S/G2/M transitions of the cell cycle.

Materials. A HybriZAP-2.1 two-hybrid predigested vector kit was purchased from Stratagene. The Fungal Genetic Stock Center (FGSC) kindly provided the conidial *N. crassa* cDNA library. A Wizard Plus Minipreps DNA purification system and restriction endonucleases were purchased from Promega. *P. pastoris* pPIC9K expression vector was from Invitrogen, pGEX-4T-1 vector was from Amersham Pharmacia Biotech, and pCITE-4a(+) vector was from Novagen. A TNT T7 coupled reticulocyte lysate system was purchased from Promega. Sephaglass FP slurry, gluthatione−Sepharose 4B matrix, L-[^{35}S]methionine, and anti-BrdU antibody were from Amersham Pharmacia Biotech. BrdU was from Sigma. Basal medium of Eagle and gentamicin were from Gibco BRL. OCT compound was from Sakura Finetek Japan. A VECTASTAIN ABC kit (mouse IgG) peroxidase system, FITC, and DAPI were purchased from Vector Labs.

Methanol-Induced High-Level Expression of rPsd1 in P. pastoris. The cDNA coding for the *Ps*d1 peptide (5 kDa) was ligated in the pPIC9K expression vector, which contains the methanol-induced *AOX1* promoter. Yeast *P. pastoris* strain GS115 was transformed with this recombinant plasmid by electroporation. After nucleotide sequencing to check the DNA constructs, the transformed strain was grown for 120 h for induction of protein expression with daily supplementation of 0.7% methanol into the medium. The recombinant protein was harvested from the culture supernatant and purified as described previously (*5*).

Yeast Two-Hybrid Interaction Screen. The conidial *N. crassa* cDNA library was a λ phage packed cDNA library constructed by the FGSC in the HybriZAP-2.1 vector with

mRNA from conidia of *N. crassa* strain 74A grown at 25 °C for 4.5 h. The cDNA were inserted in the *Eco*RI and *Xho*I unique sites of the pAD-GAL4-2.1 vector within the HybriZAP-2.1 vector.

Converting the λ packed library (titer = 10^8 cfu mL^{-1}) to the phagemid form allowed screening of the library in yeast cells. After mass excision and amplification of the excised phagemid library, *Escherichia coli* XLORL cells were infected with the phagemid library (moi = 10) in 500 mL of LB broth with 50 μg mL^{-1} ampicillin (see Stratagene's protocol). The pAD-GAL4-2.1 plasmids containing the cDNA inserts (Y_i) were purified from 500 mL of *E. coli* XLORL culture. This pool was named pAD-Y_i plasmid library, representative of the *N. crassa* target proteins. Yeast YRG-2 cells cotransformed with the pAD-Y_i plasmid library and the plasmid pBD-X encoding the bait (X = *Ps*d1) were plated on yeast synthetic dropout (SD) medium without Leu and Trp. First, the X−Y interactions were detected monitoring the expression of the *Lac*Z reporter gene by screening for β-galactosidase activity using the paper filter lift assay described below. Second, the expression of the HIS reporter gene was detected by plating blue transformants on SD medium without Leu, Trp, and His. Third, selected transformants were streaked on SD medium without Leu, Trp, and His with varying concentrations of 3-aminotriazole (3-AT). Interactions were reconfirmed by yeast cotransformation with bait and target plasmids isolated from the previously selected transformants and through growth on SD medium without Leu, Trp, and His, supplemented with 5 mM 3-AT.

Control plasmids were checked prior to the beginning of the screening experiment and concurrently with all subsequent cotransformations of YRG-2 with bait and target plasmids (see Stratagene's user manual). For assaying the expression of the *Lac*Z reporter gene, yeast transformed with pGAL4 (wild-type full-length GAL4) was the positive control, and yeast transformed with pBD-WT was the negative control. For assaying the expression of the HIS reporter gene, yeast cotransformed with pBD-WT and pAD-WT was the positive interaction control, and yeast cotransformed with pLamin C and pAD-WT was the negative interaction control.

Construction of the DNA-Binding Domain (BD) Plasmid. The cDNA encoding the plant defensin *Ps*d1 from the pPIC9K *P. pastoris* expression vector was inserted in-frame into the *Eco*RI and *Sal*I unique sites of the pBD-GAL4 Cam vector by restriction digestion. Digested pBD-GAL4 Cam vector was dephosphorylated with CIAP (calf intestine alkaline phosphatase) prior to ligation. The presence of *Ps*d1 in the bait plasmid was confirmed by digestion of the DNA isolated from XL-1 Blue MRF′ transformed colonies with *Eco*RI and *Sal*I enzymes. PCR analysis was performed using the following oligonucleotides: GAATTCATGAAGACTTGTGAACACTTAGCTGACACC for the 5′-end *Ps*d1 primer and ACAGTTTTGAGTACAGAAACACTTCCAGTCGAC for the 3′-end *Ps*d1 primer.

Measuring Psd1 Expression in pBD-Psd1 Transformed Yeast YRG-2. Expression of the plant defensin *Ps*d1 by the pBD-*Ps*d1 bait plasmid was assayed by its antifungal activity against the fungus *N. crassa*. Yeast YRG-2 transformed with pBD-*Ps*d1 was grown as a monolayer in appropriate solid medium. The cell monolayer of pBD-WT transformed YRG-2 was used as negative expression control. The fungus *N. crassa* strain 74A conidiae were applied to the center of these cell monolayers. Plates were incubated for fungus radial spread at 28 °C for 24 h.

Measuring the β-Galactosidase Activity by the Paper Filter Lift Assay. Yeast colonies were patched to SD-agar plates lacking the proper nutrients, incubated for 4 days at 30 °C, and transferred by blotting to sterile filter paper. The filters were dipped in liquid nitrogen for 10 s and returned to room temperature to allow permeabilization of the cell membrane. Filters were subsequently placed "colony side up" on the top of another filter paper that had been previously wetted with Z buffer (60 mM Na_2HPO_4, 40 mM NaH_2PO_4, 10 mM KCl, 1 mM $MgSO_4$, 50 mM β-mercaptoethanol) containing 1 mg mL^{-1} X-gal. The filters were incubated for up to 24 h at 37 °C, and blue colonies were selected (see Stratagene's protocol).

Fluorescence Microscopy Analysis. Fluorescein isothiocyanate (FITC) conjugated peptide was prepared as described previously (*17*). *F. solani* UFPe2389 strain (kindly provided by Dr. M. M. Nishikawa, INCQS, Fiocruz) was cultivated in PD medium under vigorous shaking at 27 °C for 16 h. Cell suspension was incubated with the FITC-conjugated *Ps*d1 (100 μg mL^{-1}) for 3 min or 5 h at room temperature. Cells were cytocentrifuged onto poly(L-lysine) pretreated slides, fixed in 4% paraformaldehyde, and washed twice with PBS. Nuclei staining was obtained by the addition of 500 μL of 1 μg mL^{-1} DAPI for 5 min or 50 μg mL^{-1} PI for 20 min followed by three washes with PBS. Glass coverslips were mounted on slides with 20 mM *N*-propyl gallate for further analysis of the fluorescence under a Nikon Eclipse TE300 inverted microscope. The FITC-conjugated to *Ps*d1 and the DAPI-stained nuclei localizations were revealed using B excitation (460−490 nm) for the FITC-*Ps*d1 and V excitation (330−385 nm) for DAPI at a particular field of view. Digital pictures were obtained using 60× oil-immersing objectives in a low-light cool CCD camera (CoolSNAP, Photometrics, Roper Scientific Inc.).

The E. coli Expression System and the GST Pull-Down Assay. The coding region of the insert cDNA Y_1 from plasmid pAD-Y_1 was cloned as an *Eco*RI−*Xho*I fragment into the vector pGEX-4T-1. After nucleotide sequencing to check the DNA constructs with the GST sequence, the two-hybrid potential candidate was expressed in *E. coli* BL21-(DE3) pLysS competent cells as a GST-tagged protein. Induction with IPTG was at a final concentration of 1 mM when the OD_{600nm} reached 0.5. After expression at 28 °C for 2 h in the induction medium, cells were harvested by centrifugation and disrupted by probe sonication (Branson/250) at 50 W for 5 pulses of 10 s on ice. A cleared lysate was obtained from the supernatant of centrifuged sonicated extracts. The Gluthatione−Sepharose 4B matrix was loaded with either the cleared lysate of the GST-fused protein expression or GST only from the parental pGEX-4T-1 expression as the negative control and incubated for 1 h at 4 °C. On the other hand, the *Ps*d1 gene was cloned in-frame into the vector pCITE-4a(+) as an *Eco*RI−*Sal*I fragment. The *E. coli* strain XL-1 Blue MRF′ was transformed with plasmid pCITE-*Ps*d1 and purified, and ligations were checked by restriction endonuclease digests. Both the *Ps*d1 DNA coding sequence and the luciferase T7 control DNA were used as templates for the TNT T7 coupled reticulocyte lysate system, according to the manufacturer's protocol, with

L-[^{35}S]methionine as label (data not shown). The labeled proteins were separated by SDS−PAGE, and protein bands were visualized by autoradiography. The bound GST-tagged protein Y_1, representing a potential interaction partner for the defensin *Ps*d1, was incubated for 30 min at 4 °C with the L-[^{35}S]methionine *Ps*d1 peptide. After extensive PBS washing to remove unbound proteins, the beads were resuspended in 20 μL of PBS buffer. The protein−protein interactive complexes bound to the glutathione−Sepharose 4B beads were eluted at 100 °C for 5 min and analyzed by SDS−PAGE electrophoresis followed by autoradiography.

Culture of N. crassa Filtered Conidia Cells. A two-day-old 500 mL culture in Vogel medium supplemented with 2% glucose was filtered under sterile conditions and rinsed with sterile distilled water. The mycelia pads were transferred to sterile Petri dishes, dampened with 1.5 mL of sodium phosphate buffer (0.1 M, pH 6.0), and incubated for 18−20 h at 30 °C under continuous fluorescent light. Conidia cells, intensively produced in this condition (titer higher than 10^7 cells mL^{-1}), were harvested by suspension in sterile distilled water and filtered through eight layers of sterile silk cloth (*18*). Cultures of *N. crassa* filtered conidia cells were incubated in Vogel medium supplemented with 2% glucose for 1 h at 30 °C for asynchronized germinating conidia (*19*). For a synchronized culture, 30 mM picolinic acid was added for 1 h at 30 °C to arrest cells at the G1 phase of the cell cycle. Picolinic acid treated cells were harvested by centrifugation and rinsed twice with Vogel medium supplemented with 2% glucose. Cultures were incubated for 1 h at 30 °C in this medium supplemented with 2% glucose in order to surpass the growth lag phase after removal of picolinic acid (*20*).

Flow Cytometric Analysis. Conidia obtained as described above was incubated at 30 °C in Vogel medium supplemented with 2% glucose for 30, 60, and 90 min analysis in the absence or in the presence of 80 μg mL^{-1} *Ps*d1. Cells were harvested by centrifugation and resuspended in ice-cold Vindelov solution (0.1% Triton X-100, 4.0 mM sodium citrate, 0.7 unit/mL RNase A, 50.0 μg/mL propidium iodide), kept on ice for 30 min in the dark, and then analyzed on a FACSCalibur (Becton Dickinson Immunocytometry Systems), with an argon laser tuned to 488 nm, using the Cell Quest program (BD Immunocytometry Systems). Events with high FL2-W were excluded from analysis.

Explants of Rat Retinae. Lister hooded rats at 2 days postnatal were anesthetized by hypothermia, and a solution of 5-bromo-2-deoxyuridine (BrdU, 60 mg kg^{-1}; Sigma) diluted in distilled water plus 7 mM NaOH was injected intraperitoneally. A period of 30 min was allowed after the injection of BrdU before killing the animals for histological processing. This single injection of BrdU led to the incorporation of the nucleotide into cells that were in the S phase of the cell cycle at the time of injection. Explants of rat retinae were prepared as described previously (*21*−*23*). The animals were killed painlessly, instantaneously by decapitation, and the retinae were dissected with fine forceps. Fragments of about 1 mm size were cut in culture medium and placed in 2 cm^2 plates containing 500 μL of basal medium of Eagle with 2 mM glutamine and 10 μg mL^{-1} gentamicin. The plates were kept at 37 °C for 3 h in either the presence or absence of *Ps*d1.

Immunohistochemistry. Prior to immunochemistry with anti-BrdU antibody, the explants were fixed by immersion with 4% paraformaldehyde in sodium phosphate buffer, pH 7.4 (PBS), for 1 h. After extensive PBS washes, the explants were oriented to allow a transverse cut under a dissecting microscope in an aluminum chamber filled with OCT embedding medium. OCT is a mixture of polyvinyl alcohol and polyethylene glycol that surrounds but does not infiltrate the tissue. The retina in situ was 10 μm cut frozen and mounted on slides pretreated with poly(L-lysine) (200 μg mL^{-1}). The slides were heated in citrate buffer at pH 6.0 in a microwave oven for better antigen retrieval (*24*) and incubated with 1% hydrogen peroxide for 10 min to inhibit the endogenous peroxidase background. Then, slides were incubated with 0.5% Triton X-100 in PBS for 15 min and washed with pure PBS followed by incubation with a blocking albumin solution (1% BSA in PBS) for 30 min. Incubation with the monoclonal primary anti-BrdU antibody was carried out for 1 h at room temperature. The peroxidase-based "ABC" technique from Vector Labs was used for immunohistochemical staining and detection.

Detection and Counting of Migrating Nuclei. The fraction of migrating nuclei was established on the basis of previous results showing that the S phase zone corresponds to two-thirds of the transversal dimension of the neuroblastic layer (NBL) in the developing rat retina (*25*). Thus, the nuclei labeled with BrdU which reached the outer third stratum of the NBL were scored as migrating nuclei. Nuclei were counted at 1000× magnification with differential interference contrast using an Axiophot microscope (Zeiss Inc.). Counts were made in three random 1 mm^2 fields from each of the three explants per experimental group.

RESULTS

The Yeast Two-Hybrid System To Detect Protein−Protein Interactions. To screen the fungus proteins capable of direct physical interaction with the plant defensin *Ps*d1, a GAL-4 based two-hybrid screening system using a *N. crassa* cDNA λ library was performed. The FGSC kindly provided this λ packed library, which we converted to a library in the vector pAD-GAL4-2.1. The cDNA inserts (Y_i) were cloned into the *Eco*RI and *Xho*I unique sites of the pAD-GAL4-2.1 vector. These target plasmids (pAD-Y_i) encoded *N. crassa* proteins fused to the GAL4 transcriptional activating domain (AD).

The bait plasmid was constructed by fusion of the plant defensin *Ps*d1 cDNA to the GAL4 binding-domain (BD) sequence of vector pBD-GAL4 Cam (*Eco*RI and *Sal*I unique sites) and then transformed into the yeast strain YRG-2. This plasmid, named pBD-*Ps*d1, did not activate *LacZ* or *HIS3* reporter genes by itself, confirming that *Ps*d1 is not a transcriptional activation factor of the two-hybrid system in study (data not shown). DNA sequencing by Eton Biosciences Inc., *Eco*RI and *Sal*I restriction digestion (Figure 1A), and PCR analysis with 5′-end and 3′-end *Ps*d1 primers (Figure 1B) of the bait plasmid pBD-*Ps*d1 confirmed the presence of the *Ps*d1 cDNA.

In an attempt to verify if YRG-2 containing the pBD-*Ps*d1 bait plasmid expressed the functional *Ps*d1, antifungal activity was assayed upon *N. crassa* growth on yeast monolayers. A control monolayer of YRG-2 cells containing

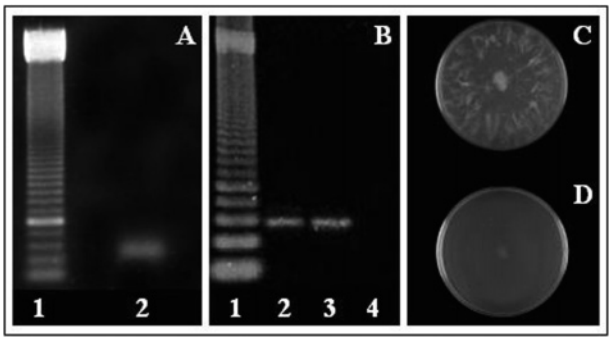

FIGURE 1: Analysis of the yeast two-hybrid bait plasmid pBD-*Ps*d1 (A) by restriction endonuclease digestion, (lane 1) standard 50 bp ladder and (lane 2) the *Eco*RI and *Sal*I fragment of *Ps*d1 cDNA (approximately 150 bp size), and (B) by PCR amplification using 5′- and 3′-end *Ps*d1 primers: (lane 1) standard 50 bp ladder, (lane 2) 150 bp fragment from pBD-*Ps*d1 bait plasmid, (lane 3) 150 bp fragment from pPIC9K-*Ps*d1 positive control, and (lane 4) pBD-GAL4 negative control. (C, D) Fungal radial growth in YRG-2 cell monolayers: (C) *N. crassa* radial growth in control monolayer not expressing *Ps*d1 and (D) monolayer of YRG-2 cells containing pBD-*Ps*d1 showing the complete growth impairment of the fungus *N. crassa*. Antifungal activity indicates expression of the fully active *Ps*d1 peptide.

pBD-WT permitted the radial spread of *N. crassa* (Figure 1C). The monolayer of pBD-*Ps*d1-transformed YRG-2 cells was protected from the fungal growth (Figure 1D). In the latter we observed a prominent fungal growth impairment, indicating the expression of fully active *Ps*d1 peptide in yeast transformed with pBD-*Ps*d1.

The yeast YRG-2, containing the two reporter *Lac*Z and HIS genes, was transformed simultaneously with the pBD-*Ps*d1 bait plasmid and the *N. crassa* cDNA library. Yeast transformants in SD selective medium depleted of Leu and Trp were identified by β-galactosidase activity as the first criterion for screening protein−protein interactions (Figure 2, first criterion). Fifteen blue transformants were detected expressing the *Lac*Z reporter gene. As the two-hybrid interaction second criterion, these 15 blue transformants were streaked on SD agar lacking Leu, Trp, and His (His-selective medium), confirming the 15 strong interactions by the expression of the HIS3 reporter gene (Figure 2, second criterion). Target colonies were selected again on HIS selective medium with varying concentrations of 3-AT, as the third criterion (Figure 2, third criterion). 3-AT inhibits any leaky expression of the His reporter gene. As shown by the literature, 3-AT concentrations of less than or equal to 5 mM were not toxic to YRG-2 cells (*26*−*28*). Despite showing some level of toxicity to YRG-2 cells, some stronger interactions could be differentiated with 3-AT concentrations higher than 15 mM (data not shown). To reconfirm interactions, cotransformations of yeast YRG-2 with the plant defensin *Ps*d1 bait vector and with each of the 15 plasmids isolated from the candidates that grew on HIS-selective medium with 5 mM 3-AT were performed individually as the fourth criterion (Figure 2, fourth criterion). Yeast containing these selected inserts resulted in the expression of the HIS3 reporter gene in the presence of 5 mM 3-AT, identifying 15 two-hybrid candidates. These candidates are strong as the two-hybrid positive interaction control (Figure 2, C1). The negative interaction control does not grow on SD agar depleted of Leu, Trp, and His, supplemented or not with 3-AT (Figure 2, C2).

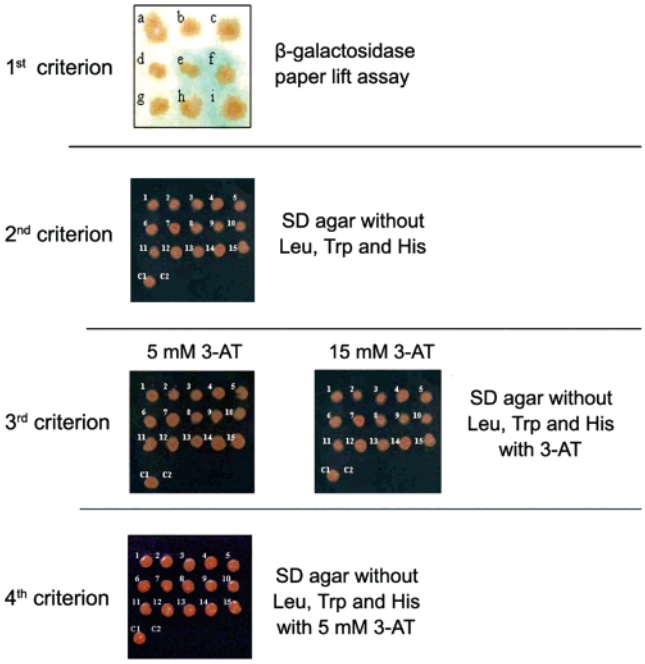

FIGURE 2: Two-hybrid system analysis. First criterion: The expression of the *Lac*Z reporter gene detected by the paper filter lift assay. Blue colonies (e, f, h, and i) are shown as an example of colonies inducing β-galactosidase, therefore two-hybrid candidates. Second criterion: The expression of the HIS3 reporter gene in 15 colonies selected using the first criterion. Third criterion: The expression of the HIS3 reporter gene supplemented with 5 and 15 mM 3-AT. Fourth criterion: The cotransformation of the bait plasmid pBD-*Ps*d1 and each of the pAD-Yi plasmids ($i = 1-15$). The 15 two-hybrid candidates are shown followed by the positive (C1) and the negative (C2) interaction controls.

All 15 candidates had their target plasmids isolated and sequenced by Eton Biosciences Inc. Sequences were analyzed by MIPS WU-BLAST 2.0 similarity search against *N. crassa* databases (http://mips.gsf.de/cgi-bin/blast/blast_page?genus=Ncrassa).

As shown in Table 1, 11 out of the 15 candidates exhibited BLASTN and/or BLASTX similarities to *N. crassa* nucleotide and protein sequences databases. Nine out of 11 candidates presented BLASTX sequence similarities to nuclear proteins. The cDNA inserts Y_1, Y_2, and Y_{15} (Table 1) repeated the same MIPS BLASTN and BLASTX sequence database search, three times out of 15 candidates. The identification of the same cDNA target insert in three interactions per library screening reduced considerably the false negative rate.

Agarose gel analysis of clones Y_1, Y_2, and Y_{15} showed the DNA sizes around 3 kb as predicted by BLASTX results (data not shown). These sequences demonstrated similarities with close expectation and probability numbers to the same sequence encoding a protein related to the *N. crassa* cell cycle control. It was classified as Whitehead code NCU04540.1/MIPS entry 4nc448_040 (retrieve sequences at http://pedant. gsf.de/cgi-bin/wwwdbp.pl?Db=Ncrassa_annotations&Alias=Ncrassa_ANNOTATIONS&Name=dyn-rep&String=7638&Title=Ncrassa_ANNOTATIONS&Contig=LGIV:4nc448&ContigId=359&Cmd=Fetch). It coded for a *N. crassa* cyclin-like protein, with the F-box and WD-repeat domain, related to the cell cycle control. Its closest SIMAP fungi homologue is the hypothetical protein Uniprot accession number Q2GPF9 of fungus *Chaetomium globosum* CBS

Table 1: Fifteen Two-Hybrid Candidates Y_i ($i = 1-15$)[a]

two-hybrid candidates	BLASTN *e*-value	BLASTX *e*-value	list of ORFs	protein localization	protein function	length (aa)
Y_1, Y_2, and Y_{15}	2.3e−41	0.14	4nc448 040	nuclear	cyclin F-box WD domain	1010
Y_3	2.6e−92	0.95	29e8 260	nuclear	Zn-finger-like PHD finger	948
Y_4 and Y_7	3.4e−49	0.0064	7nc605 250	plasma membrane	unknown	683
Y_5		0.97	2nc610 340	nuclear	Uni-Zap clone A1H06NP5′	713
Y_6	0.00064	0.15	3nc310 110	nuclear	unknown	103
Y_8	1.0e−48	0.05	1nc400 220	nuclear	hypothetical protein similar to YGR280c	369
Y_9	1.1e−32	1.4e−23	b16b8 350	nuclear	unknown	587
Y_{10}, Y_{11}, Y_{13}, and Y_{14}			none[b]			
Y_{12}	8.4e−26	0.36	4nc570 330	nuclear	Uni-Zap clone C1D03NP5′	518

[a] Sequences were analyzed by the MIPS WUBLAST 2.0 similarity search against *N. crassa* databases (http://mips.gsf.de/cgi-bin/blast/blast_page?genus=Ncrassa). [b] No sequence similarities in *N. crassa* databases.

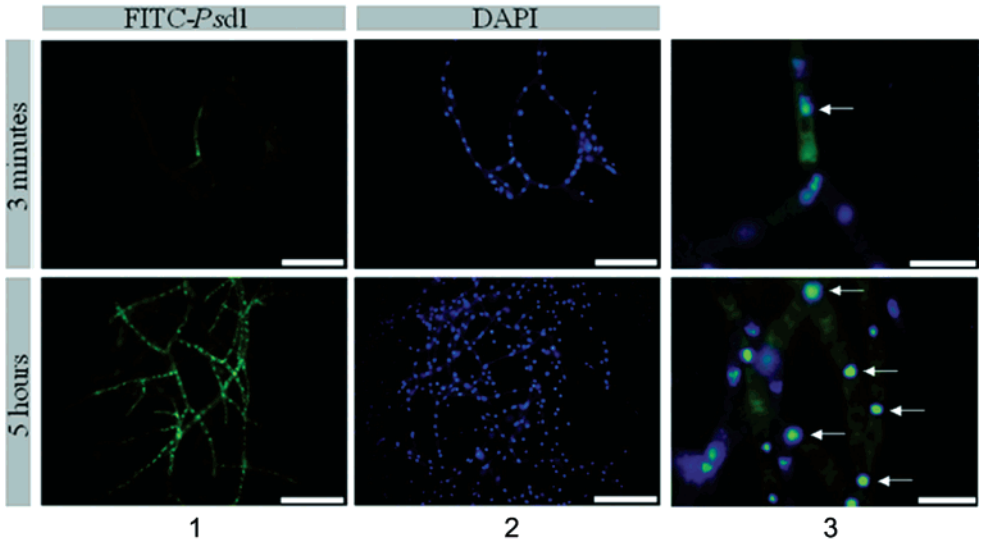

FIGURE 3: Fluorescence microscopic analysis of FITC-conjugated *Ps*d1 and DAPI-stained nuclei. (Lane 1) *F. solani* hyphae were incubated for 3 min or 5 h with 20 μM FITC-conjugated *Ps*d1 (green fluorescence). (Lane 2) After this incubation period, the nuclei were stained with DAPI (blue fluorescence). (Lane 3) The white arrows show colocalization of *Ps*d1 and the fungus nuclei. Bars represent 50 μm (lanes 1 and 2) and 10 μm (lane 3).

148.51 with 64.27% similarity (51.05% identity). Also, SIMAP database analysis provides the information that *N. crassa* cyclin F protein has sequence similarities with mammalian F-box/WD-repeat proteins: 53.99% similarity (35.80% identity) to human F-box/WD-repeat protein 1A Uniprot accession number Q9Y297 and 53.8% similarity (35.85% identity) to *Cannis familiaris* F-box/WD-repeat protein 1A NCBI accession number XP_861929. Moreover, it has 53.99% similarity (35.81% identity) to *Bos taurus* F-box/WD-repeat protein 1A NCBI accession number XP613703 (SIMAP analysis at http://mips.gsf.de/genre/proj/ncrassa/singleGeneReport.html?entry=4nc448_040).

Two other candidates, Y_4 and Y_7 (Table 1), presented BLASTN and BLASTX sequence similarities with very close expectation and probability numbers to the same *N. crassa* nucleotide sequences. These inserts represented a hypothetical protein localized on the fungal plasma membrane with 115 amino acids targeting signal to mitochondria. These clones should be restudied with a membrane-based yeast two-hybrid system.

The other two-hybrid candidates Y_3, Y_5, Y_6, Y_8, Y_9, and Y_{12} (Table 1) coded for nuclear proteins. The insert Y_3 had the highest probability similarity to a *N. crassa* nucleotide sequence (BLASTN *e*-value = 2.6e−92), encoding a zinc-finger protein that has the ability to bind to both RNA and DNA. Inserts Y_5 and Y_{12} have unknown nuclear functions. These inserts have already been detected in other Uni-Zap clones. Insert Y_9 had the highest probability similarity to a *N. crassa* amino acid sequence (BLASTX *e*-value = 1.4e−23), encoding an unknown nuclear protein. Since several two-hybrid candidates encoded nuclear proteins, the plant defensin *Ps*d1 is probably internalized into the fungal cytoplasm toward the nucleus.

Fluorescence Microscopy of FITC-Psd1 and DAPI-Stained F. solani Nuclei. We have previously demonstrated that very low concentrations of *Ps*d1 peptide were required for 50% growth inhibition of fungi *F. solani* and *N. crassa* (*4*). In order to verify the ability of peptide *Ps*d1 to enter the fungus cells and to localize to the nuclei in vivo, the fluorophores FITC conjugated to *Ps*d1 peptide (green color) and DAPI intercalating DNA dye (blue color) were applied sequentially to the growing hyphae of *F. solan*i. Fluorescence microscopic images of the FITC-conjugated *Ps*d1 peptide and the DAPI-stained nuclei were captured separately with a coupled device camera (Figure 3). The FITC-conjugated *Ps*d1 peptide demonstrated that *Ps*d1 was internalized into *F. solani* hyphae (Figure 3, lane 1). The DAPI stain revealed the position of several numbers of nuclei present in the *F. solani* hyphae (Figure 3, lane 2). The images taken with *Ps*d1 treated for 3 min or 5 h and with DAPI-stained hyphae were

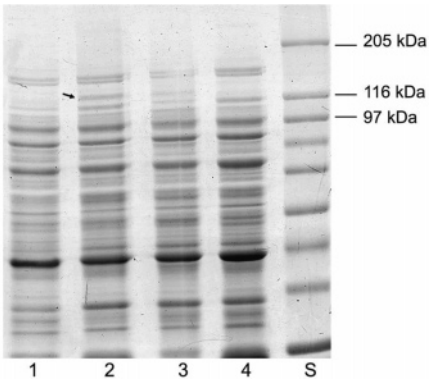

FIGURE 4: Expression of the two-hybrid candidate Y_1 fused to GST in the *E. coli* BL21(DE3) pLysS system. (Lane 1) The zero-time induction. (Lane 2) The 2 h expression in the presence of 1 mM IPTG. (Lane 3) The 2 h expression in the absence of IPTG. (Lane 4) The parental pGEX-4T-1 2 h expression in the presence of 1 mM IPTG. The arrow (lane 2) points to the GST-fused two-hybrid candidate protein Y_1 (approximately 140 kDa).

superimposed for fluorophore colocalization analysis. As illustrated by Figure 3 (lane 3), the FITC-conjugated *Ps*d1 peptide colocalized with the DAPI-stained nuclei in *F. solani* hyphae. The above result confirmed that *Ps*d1 targeted the fungal nucleus.

Expression of the Two-Hybrid Candidate Y_1 Fused to GST in E. coli. The sequence named Y_1 that resulted in the highest probability of interaction on the two-hybrid screening with sequence similarity to a *N. crassa* known cyclin F protein was studied further. The target protein Y_1 fused to the GST tag in the pGEX-4T-1 expression vector was expressed in *E. coli* BL-21(DE3) pLysS IPTG-induced competent cells following sonication and centrifugation to yield a cleared lysate. The expression products were analyzed by SDS−PAGE. As shown in Figure 4, one new protein band of molecular mass around 140 kDa became visible after 2 h of IPTG-induced expression in *E. coli* BL-21(DE3) pLysS competent cells (Figure 4, lane 2, the black arrow). This protein was not observed in the zero time control (Figure 4, lane 1) or in the 2 h expression of the parental empty vector (Figure 4, lane 4). The molecular mass of this particular polypeptide product matched the expected theoretical value for the candidate cyclin F, 4nc448_040 (111481 Da) plus GST (27000 Da).

In Vitro Verification of the Interaction by the GST Pull-Down Assay. The plant defensin *Ps*d1 DNA was transferred from the bait plasmid pBD-*Ps*d1 into the *Eco*RI and *Sal*I unique sites of the pCITE-4a(+) expression vector, and the L-[^{35}S]methionine labeled *Ps*d1 was expressed in the reticulocyte lysate system (Figure 5, lane 1).

Gluthatione−Sepharose 4B beads were loaded with the cleared lysate containing the GST-fused *N. crassa* protein Y_1 (+) or the GST only negative control (−) and incubated with the L-[^{35}S]methionine-labeled *Ps*d1. Following extensive washes, the bound proteins were eluted by denaturation, separated on SDS−PAGE, and analyzed by autoradiography.

As shown in Figure 5 (lane 2), the L-[^{35}S]methionine defensin *Ps*d1 interacted in vitro with the *N. crassa* two-hybrid candidate cyclin F, related to the cell cycle control. GST by itself did not interact with the L-[^{35}S]methionine-labeled *Ps*d1 (Figure 5, lane 3).

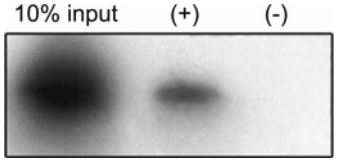

FIGURE 5: GST pull-down assay. (Lane 1) 10% input of L-[^{35}S]-methionine-labeled *Ps*d1 expressed in the TNT T7 coupled reticulocyte lysate system. (Lane 2) The in vitro interaction of the GST-tagged two-hybrid protein Y_1 and the L-[^{35}S]methionine-labeled *Ps*d1 (plus sign). (Lane 3) The GST only and the L-[^{35}S]methionine-labeled *Ps*d1 as the negative interaction control (minus sign). Either the GST-tagged protein Y_1 or the GST only bounded to the Gluthatione−Sepharose 4B beads was incubated with the L-[^{35}S]-methionine-labeled *Ps*d1. After extensive washes, the protein−protein interactive complexes were eluted by denaturation and analyzed by SDS−PAGE electrophoresis and then by autoradiography.

For the first time, we found a direct physical interaction of the plant peptide *Ps*d1 with an intracellular protein, a *N. crassa* cyclin F, one of the largest in the cyclin family.

Psd1 Affects the Cell Cycle of N. crassa Conidia. In order to verify if *Ps*d1 interfered in the cell cycle progression of *N. crassa* germinating conidia, we measured the conidial DNA content by flow cytometry (Figure 6). The synchronized conidia population arrested in G1 showed a well-defined peak observed within 30, 60, and 90 min treatment with 80 μg mL^{-1} *Ps*d1. While this characteristic peak diminished, the DNA content increased with time in the presence of *Ps*d1, as demonstrated by the appearance of a conidia population with higher fluorescence intensity (Figure 6A). Control cells treated with picolinic acid, in the absence of *Ps*d1 peptide, did not show this fluorescence pattern shift (Figure 6B). Fluorescence microscopic analysis of DAPI or PI nuclei conidia showed the presence of multinucleated cells (data not shown). Taking into account that the duration of the cell cycle in *N. crassa* is 100 min in glucose-supplemented medium (*29*), this DNA rereplication is probably occurring before a succeeding mitosis, suggesting that this defensin interferes with *N. crassa* nuclear division and affects the cell cycle. Monitoring the asynchronized cell population by FACS also showed that the DNA content had shifted to higher fluorescence in the presence of *Ps*d1 (data not shown).

Psd1 Peptide Impairs Nuclear Migration in Neuroblasts of the Rat Retina. Since the levels of cyclin F are highly regulated during progression along the S/G2/M phases of the cell cycle (*14*, *15*), we speculated that *Ps*d1 could affect the cell cycle during this period. Phase transitions in the nervous system are easily monitored by nuclear position within the elongated proliferating cells, a property called interkinetic nuclear migration. During interkinetic nuclear migration, DNA is duplicated in the innermost margin (S phase zone), while mitosis occurs in the outermost margin of the neuroblastic layer (*24*, *25*).

To evaluate the effects of *Ps*d1 upon the cell cycle, proliferating cells at S phase were pulse labeled with BrdU in vitro. Retinal explants were then treated with *Ps*d1 for 3 h. This time allowed cells to end S phase, pass through G2 phase, and enter mitosis but not to progress along the G1 phase of a new cell cycle. The BrdU-labeled nuclei that reached the outer third stratum of the neuroblastic layer (NBL) were scored as migratory nuclei.

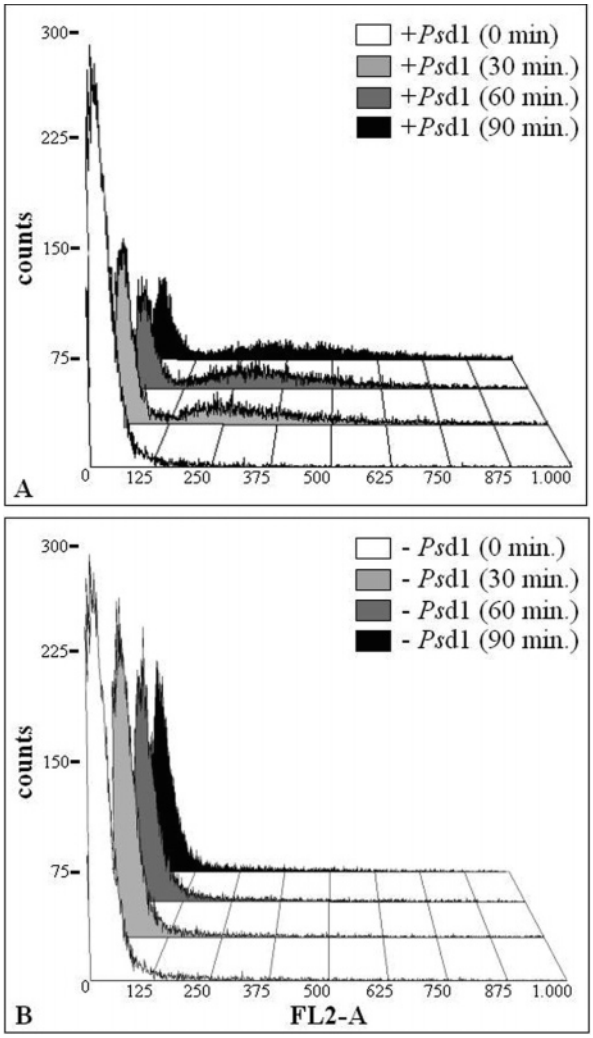

FIGURE 6: Effect of *Ps*d1 on the DNA content of *N. crassa* germinating conidia. Synchronized conidia were incubated at 30 °C for different times: (A) in the presence of 80 μg mL^{-1} *Ps*d1 and (B) in the absence of *Ps*d1 peptide. Conidia were analyzed by flow cytometry after staining with a propidium iodide- and RNase-containing solution.

Analysis of the interkinetic nuclear migration along the NBL showed that treatment with *Ps*d1 inhibited migration of retina neuroblast nuclei (Figure 7, panel A compared with panel B). The inhibition of nuclear migration by *Ps*d1 was dose-dependent in this model (Figure 7C). At 80 μg mL^{-1} *Ps*d1, 50% of nuclei reached the outermost margin of the NBL and were scored as migrating nuclei. This result showed that *Ps*d1 disturbs nuclear migration in the mammalian retinal tissue. We did not detect apoptotic profiles labeled with BrdU (*21*), showing that *Ps*d1 did not induce the death of proliferating cells under these conditions.

DISCUSSION

In this study, the yeast two-hybrid screening system was used to identify *N. crassa* proteins, which directly interacted with the plant defensin *Ps*d1 from garden pea. Nine out of 11 candidates presented sequence similarities to nuclear proteins (Table 1). Among the nuclear proteins identified by the two-hybrid system, there was a *N. crassa* F-box/WD-repeat cyclin-like protein 4nc448_040 with functional categories in the mitotic cell cycle and cell cycle control, which was detected with a high frequency per screening.

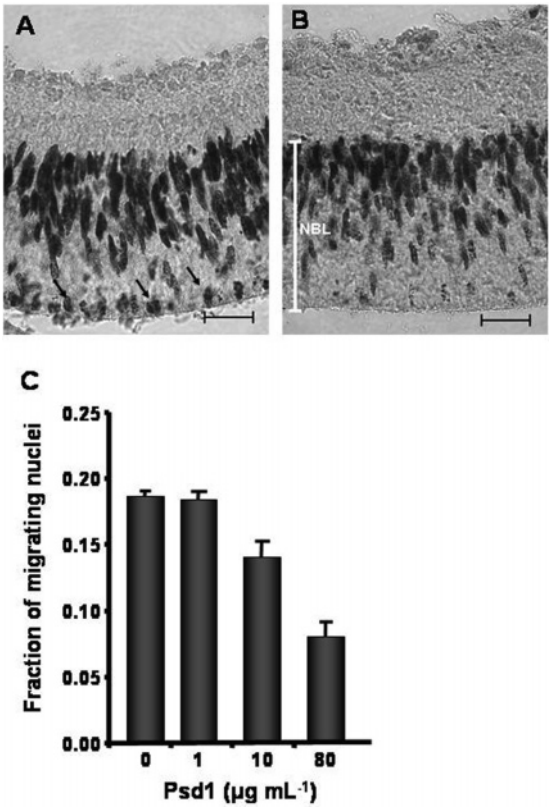

FIGURE 7: Measurement of the interkinetic nuclear migration along the neuroblastic layer (NBL) in the developing rat retina. (A) In the absence of *Ps*d1, immunohistochemistry using anti-BrdU antibody shows that nuclei labeled with BrdU proceed in synchrony toward the outermost stratum (lower base). The black arrows indicate nuclei at the lower base of the NBL. (B) In the presence of 80 μg mL^{-1} *Ps*d1, the interkinetic nuclear migration was impaired at the S to G2 phase transition. The white bar indicates the NBL. (C) The interkinetic nuclear migration measured by the fraction of migrating BrdU-labeled nuclei that reached the outermost third stratum of the NBL is *Ps*d1 dose-dependent. The concentration of 80 μg mL^{-1} *Ps*d1 estimates 50% inhibition. The black bars = 20 μm.

Bioinformatic analysis revealed highly conserved domains among cyclin F sequences, indicating the possibility of crossed interactions between *Ps*d1 and related cell cycle F-box/WD-repeat proteins of other species. GST pull-down assay confirmed the in vitro binding between *Ps*d1 and *N. crassa* cyclin F (Figure 5). This physical interaction can be regarded as a new tool to study the function of cyclin F in the cell cycle. So far, no cyclin-dependent kinase partner has been identified to human cyclin F, which is called an "orphan" cyclin (*14*).

Due to the highly conserved cell cycle machinery, researchers interested in the regulation of cell proliferation moved away from single-cell model systems such as yeast to examine the regulation of cell division during the development of multicellular organisms (*30*). To study the role of the interaction between *Ps*d1 and cyclin F, the developing retinal tissue of neonatal rats proved to be an ideal model since the S to G2 phase transition and the G2 to M phase transition periods correspond exactly to the cyclin F expression profile during the cell cycle (*14*). In this neural system for each round of cell division DNA synthesis in the S phase occurs when the nucleus is in the inner surface area of the NBL, and cell cycle progression from S to M phase occurs as the nucleus migrates toward the outermost rim of

the NBL (*24*, *25*). The present work demonstrated that the antifungal peptide *Ps*d1 impaired the progression of the cell cycle, as measured by interkinetic nuclear migration in the retinal neuroblasts (Figure 7). The data presented herein are consistent with the hypothesis that *Ps*d1 regulates nuclear migration by blocking the roles of cyclin F in the S to G2 phase transition of the cell cycle.

Nuclear migration has been studied during migration of daughter nucleus in yeast, during the migration of nuclei to the tip of filamentous fungi hyphae, and during migration to cortex in fly development as well as during specific migrations in worm development (*31*). Similarities between the NUDF nuclear migration protein of *Aspergillus nidulans* and human LIS1, a protein required for neuronal migration in the developing brain, suggest conserved functions and mechanisms (*32*).

Tubulin *A. nidulans* mutants provided insights that both intranuclear and cytoplasmic microtubules (MTs) are crucial for nuclear migration and cell division in filamentous fungus (*33*, *34*). Indeed, MTs in *Candida albicans* are involved in positioning the hyphal nuclei and connect cell cycle progression to hyphal elongation (*35*). Nonetheless, the intertwinement of the cell cycle transitions, nuclear migration, cytoskeletal MTs, and hyphal elongation in filamentous fungus is unclear. It has been shown that the antifungal peptide auristatin PHE, a synthetic derivative of the marine dolastatin 10 peptide, completely inhibited nuclear migration and cell division in *Cryptococcus neoformans* accompanied by as well as provoking microtubule disruption (*36*). These findings pointed to the possibility that *Ps*d1 caused the disruption of the microtubule network, therefore blocking nuclear migration. However, our results indicated that this is not the case, since *Ps*d1 seemed not to disturb nuclear distribution in *F. solani* hyphae either by nuclear clustering or by aberrant empty hyphal extensions. In fact, DAPI-stained *F. solani* nuclei pretreated with *Ps*d1 for 5 h, as revealed in Figure 3 (lane 2), showed normally spaced nuclei distribution along the fungus hyphae.

Whether *Ps*d1 affects MTs dynamics remains unclear. It is possible that cyclin F is linked to cytoskeletal MTs, since it has been reported that cyclin F transports cyclin B1 (which lacks nuclear localization domains) into the nucleus during the G2 to M phase transition (*37*). Therefore, the hypothesis that *Ps*d1 binding to cyclin F leads to impairment of cyclin B1 nuclear translocation and cell cycle arrest should be investigated in the future.

Cyclin B1 plays an important role as a component of the maturation/mitosis-promoting factor in the G2 to M phase transition during the cell cycle (*38*). Since overexpression of cyclin B1 has been extensively reported in various malignant tumor cells (*39*−*42*), it is also possible that *Ps*d1 may eventually prove to be useful as a therapeutic peptide to impair cell cycle progression and uncontrolled tumor proliferation. It remains to be investigated whether the interaction between *Ps*d1 and cyclin F interferes with the interaction between the cyclins F and B1.

Wuarin and co-workers (*43*) demonstrated that synchronized populations of fission yeast cells lacking mitotic cyclin B/Cdc2 (Cdk1) kinase undergo complete, distinct, and successive rounds of S phase without an intervening mytosis. Futhermore, they argued that stable association of mitotic cyclin B/Cdc2 kinase to replication origins might be the primary mechanism by which the order of S phase and M phase is maintained during the mitotic cell cycle. On the basis of the two-hybrid experiment and FACS analysis on *N. crassa* germinating conidia described in this paper and according to Wuarin and co-workers (*43*), we propose that the interaction between *Ps*d1 and cyclin F interferes, destabilizing the association of mitotic cyclin B/Cdc2 kinase to replication origins. Therefore, this interference should promote endoreduplication as observed in this work (Figure 6) by the analysis of *N. crassa* DNA content in the presence of *Ps*d1 peptide.

ACKNOWLEDGMENT

The authors thank R. M. Domingues for technical assistance and M. S. Almeida and T. Domitrovic for valuable help and discussions. We also thank Drs. V. Moura-Neto, A. Hemerly, and A. Nóbrega for the use of their laboratory facilities. Finally, we thank L. E. Díaz Giménez for the table of contents graphic.

REFERENCES

1. Thomma, B. P. H. J., Cammue, B. P. A., and Thevissen, K. (2003) Mode of action of plant defensins suggests a therapeutic potential, *Curr. Drug Targets: Infect. Disord. 3*, 1−8.
2. Thomma, B. P. H. J., Cammue, B. P. A., and Thevissen, K. (2002) Plant defensins, *Planta 216*, 193−202.
3. Broekaert, W. F., Cammue, B. P. A., Thevissen, K., De Samblanx, G. W., and Osborn, R. W. (1997) Antimicrobial peptides from plants, *Crit. Rev. Plant Sci. 16*, 297−323.
4. Almeida, M. S., Cabral, K. M. S., Zingali, R. B., and Kurtenbach, E. (2000) Characterization of two novel defense peptides from pea (*Pisum sativum*) seeds, *Arch. Biochem. Biophys. 378*, 278−286.
5. Cabral, K. M. S., Almeida, M. S., Valente, A. P., Almeida, F. C. L., and Kurtenbach, E. (2003) Production of the active antifungal *Pisum sativum* defensin 1 (Psd1) in *Pichia pastoris*: overcoming the inefficiency of the STE13 protease, *Protein Expression Purif. 31*, 115−122.
6. Almeida, M. S., Cabral, K. M. S., Kurtenbach, E., Almeida, F. C. L., and Valente, A. P. (2002) Solution structure of *Pisum sativum* defensin 1 by high resolution NMR: plant defensins, identical backbone with different mechanisms of action, *J. Mol. Biol. 315*, 749−757.
7. Ferket, K. K. A., Levery, S. B., Cammue, B. P. A., and Thevissen, K. (2003) Isolation and characterization of *Neurospora crassa* mutants resistant to antifungal plant defensins, *Fungal Genet. Biol. 40*, 176−185.
8. Thevissen, K., Ghazi, A., De Samblanx, G. W., Brownlee, C., Osborn, R. W., and Broekaert, W. F. (1996) Fungal membrane responses induced by plant defensins and thionins, *J. Biol. Chem. 272*, 32176−32181.
9. Thevissen, K., Terras, F. R. G., and Broekaert, W. F. (1999) Permeabilization of fungal membranes by plant defensins inhibits fungal growth, *Appl. Environ. Microbiol. 65*, 5451−5458.
10. Thevissen, K., Ferket, K. K. A., François, I. E. J. A., and Cammue, B. P. A. (2003) Interactions of antifungal plant defensins with fungal membrane components, *Peptides 24*, 1705−1712.
11. Thevissen, K., Cammue, B. P., Lemaire, K., Winderickx, J., Dickson, R. C., Lester, R. L., Ferket, K. K., Van Even, F., Parret, A. H., and Broekaert, W. F. (2000) A gene encoding a sphingolipid biosynthesis enzyme determines the sensitivity of *Saccharomyces cerevisiae* to an antifungal plant defensin from dahlia (*Dahlia merckii*), *Proc. Natl. Acad. Sci. U.S.A. 97*, 9531−9536.
12. Aerts, A. M., François, I. E. J. A., Bammens, L., Cammue, B. P. A., Smets, B., Winderickx, J., Accardo, S., De Vos, D. E., and Thevissen, K. (2006) Level of M(IP)2C sphingolipid affects plant defensin sensitivity, oxidative stress resistance and chronological life-span in yeast, *FEBS Lett. 580*, 1903−1907.
13. Thevissen, K, Warnecke, D. C., Francois, I. E., Leipelt, M., Heinz, E., Ott, C., Zahringer, U., Thomma, B. P., Ferket, K. K., and Cammue, B. P. (2004) Defensins from insects and plants interact with fungal glucosylceramides, *J. Biol. Chem. 279*, 3900−3905.

14. Bai, C., Richman, R., and Elledge, S. J. (1994) Human cyclin F, *EMBO J. 13*, 6087−6098.
15. Arooz, T., Yam, C. H., Siu, W. Y., Lau, A., Li, K. K. W., and Poon, R. Y. C. (2000) On the concentrations of cyclins and cyclin-dependent kinases in extracts of cultured human cells, *Biochemistry 39*, 9494−9501.
16. Campos, C. B. L., Bédard, P. A., and Linden, R. (2002) Activation of p38 mitogen-activated protein kinase during normal mitosis in the developing retina, *Neuroscience 112*, 583−591.
17. Lee, D. G., Kim, P. I., Park, Y., Park, S.-C., Woo, E.-R., and Hahm, K.-S. (2002) Antifungal mechanism of SMAP-29 (1-18) isolated from sheep myeloid mRNA against *Trichosporon beigelii*, *Biochem. Biophys. Res. Commun. 295*, 591−596.
18. Martegani, E., Tomè, F., and Trezzi, F. (1981) Timing of nuclear division cycle in *Neurospora crassa*, *J. Cell Biol. 48*, 127−136.
19. Serna, L., and Stadler, D. (1978) Nuclear division cycle in germinating conidia of *Neurospora crassa*, *J. Bacteriol. 136*, 341−351.
20. Martegani, E., Levi, M., Trezzi, F., and Albergina, L. (1980) Nuclear division cycle in *Neurospora crassa* hyphae under different growth conditions, *J. Bacteriol. 142*, 268−275.
21. Rehen, S. K., Varella, M. H., Freitas, F. G., Moraes, M. O., and Linden, R. (1996) Contrasting effects of protein synthesis inhibition and of cyclic AMP on apoptosis in the developing retina, *Development 122*, 1439−1448.
22. Rehen, S. K., Neves, D. D. C., Fragel-Madeira, L., Britto, L. R. G., and Linden, R. (1999) Selective sensitivity of early post-mitotic retinal cells to apoptosis induced by inhibition of protein synthesis, *Eur. J. Neurosci. 11*, 4349−4356.
23. Araujo, E. G., and Linden, R. (1993) Trophic factors produced by retinal cells increase the survival of retinal ganglion cells in vitro, *Eur. J. Neurosci. 5*, 1181−1188.
24. Dover, R., and Patel, K. (1994) Improved methodology for detecting bromodeoxyuridine in cultured cells and tissue sections by immunocytochemistry, *Histochem. Cell Biol. 102*, 383−387.
25. Hayes, N. L., and Nowakowski, R. S. (2000) Exploiting the dynamics of S-phase tracers in the developing brain: interkinetic nuclear migration for cells entering versus leaving the S-phase, *Dev. Neurosci. 22*, 44−55.
26. Faure′, J.-D., Gingerich, D., and Howell, S. H. (1978) *Arabidopsis* immunophilin, AtFKBP12, binds to AtFIP37 (FKBP interacting protein) in an interaction that is disrupted by FK506, *Plant J. 15*, 783−789.
27. Ssoellick, T.-R., Uhring, J. F., Bucher, G. L., Kellmann, J.-W., and Schreier, P. H. (2000) The movement protein NSm of tomato spotted wilt tospovirus (TSWV): RNA binding, interaction with the TSWV N protein, and identification of interacting plant proteins, *Proc. Natl. Acad. Sci. U.S.A. 97*, 2373−2378.
28. Ohkura, N., Ohkubo, T., Maruyama, K., Tsukada, T., and Yamaguchi, T. (2001) The orphan nuclear receptor NOR-1 interacts with the homeobox containing protein Six3, *Dev. Neurosci. 23*, 17−24.
29. Albergina, L., and Sturani, E. (1981) Control of growth and of the nuclear division cycle in *Neurospora crassa*, *Microbiol. Rev. 45*, 99−122.
30. Dyer, M. A., and Cepko, C. L. (2001) Regulating proliferation during retinal development, *Nat. Rev. Neurosci. 2*, 333−342.
31. Morris, N. R. (2000) Nuclear migration: from fungi to the mammalian brain, *J. Cell Biol. 148*, 1097−1101.
32. Xiang, X., Osmani, A. H., Osmani, S. A., and Morris, N. R. (1995) NudF, a nuclear migration gene in *Aspergillus nidulans*, is similar to the human LIS-1 gene required for neuronal migration, *Mol. Biol. Cell 6*, 297−310.
33. Oakley, B. R., and Morris, N. R. (1981) A beta-tubulin mutation in *Aspergillus nidulans* that blocks microtubule function without blocking assembly, *Cell 24*, 837−845.
34. Willins, D. A., Xiang, X., and Morris, N. R. (1995) An alpha tubulin mutation suppresses nuclear migration mutations in *Aspergillus nidulans*, *Genetics 141*, 1287−1298.
35. Finley, K. R., and Berman, J. (2005) Microtubules in *Candida albicans* hyphae drive nuclear dynamics and connect cell cycle progression to morphogenesis, *Eukaryot. Cell 4*, 1697−1711.
36. Woyke, T., Roberson, R. W., Pettit, G. R., Winkelmann, G., and Pettit, R. K. (2002) Effect of Auristatin PHE on microtubule integrity and nuclear localization in *Cryptococcus neoformans*, *Antimicrob. Agents Chemother. 46*, 3802−3808.
37. Kong, M., Barnes, E. A., Ollendorff, V., and Donoghue, D. J. (2000) Cyclin F regulates the nuclear localization of cyclin B1 through a cyclin-cyclin interaction, *EMBO J. 19*, 1378−1388.
38. Norbury, C., and Nurse, P. (1992) Animal cell cycles and their control, *Annu. Rev. Biochem. 61*, 441−470.
39. Yoshida, T., Tanaka, S., Mogi, A., Shitara, Y., and Kuwano, H. (2004) The clinical significance of Cyclin B1 and Wee1 expression in non-small-cell lung cancer, *Ann. Oncol. 15*, 252−256.
40. Yasuda, M., Takesue, F., Inutsuka, S., et al. (2002) Overexpression of cyclin B1 in gastric cancer and its clinicopathological significance: an immunohistological study, *J. Cancer Res. Clin. Oncol. 128*, 412−416.
41. Takeno, S., Noguchi, T., Kikuchi, R., et al. (2002) Prognostic value of cyclin B1 in patients with esophageal squamous cell carcinoma, *Cancer 94*, 2874−2881.
42. Soria, J. C., Jang, S. J., Khuri, F. R., et al. (2000) Overexpression of cyclin B1 in early-stage non-small cell lung cancer and its clinical implication, *Cancer Res. 60*, 4000−4004.
43. Wuarin, J., Buck, V., Nurse, P., and Millar, J. B. A. (2002) Stable association of mitotic cyclin B/Cdc2 to replication origins prevents endoreduplication, *Cell 111*, 419−431.

BI061441J